

53-36
46515 ~~0283~~
N91-71746
R.D.

DATA RETRIEVAL IN LASER ANEMOMETRY
BY DIGITAL CORRELATION

SV885390

by

A. E. Smart
Spectron Development Laboratories, Inc.
3303 Harbor Boulevard, Suite G-3
Costa Mesa, CA 92626

Presented at:

Third International Workshop on Laser Velocimetry
Purdue University, July 11-13, 1978

DATA RETRIEVAL IN LASER ANEMOMETRY
BY DIGITAL CORRELATION

A. E. SMART

Spectron Development Laboratories, Inc.
3303 Harbor Blvd., Suite G-3
Costa Mesa, California 92626

ABSTRACT

In hostile environments the price of good signal quality is often very high in terms of engineering or complexity. It is therefore more cost effective to use a subtle approach to interpret a small signal than to guarantee a larger signal. Acceptance of this view gives other advantages such as suitability of smaller particles, tolerance of smaller windows and easier use of backscatter. The satisfactory retrieval of data from signals which are reduced from the classical plus noise to shot noise dominated or even photon resolved may be achieved by using correlation. The high-speed electronics now available make this technique suitable for real fringe or transit anemometry. Digital correlation is an optimal method for acquiring measurements from a transit system whose ability to operate successfully close to walls is now widely accepted. Data are presented to show the advantages of this retrieval method in some difficult measurement cases, such as rotating machinery and aero-engine exhausts.

NOTATION

c	Hyperbolic attenuation with z
d	Spot separation
l_o	$1/e^2$ intensity radius for fringe system
r	Fringe contrast
s	Sampling space
x,y,z	Cartesian coordinates
θ	Half angle of beam intersection for fringes
W_o	$1/e^2$ intensity radius of spot at $z = 0$
λ	Wavelength of illumination
$I_{f(s)}$	Intensity in fringe system
$I_{t(s)}$	Intensity in two-spot system

INTRODUCTION

Laser anemometry is very broadly the measurement of velocity by detecting and decoding the light scattered from small particles. In the early days of this technology, heavy stress was placed on reference beam and then fringe optical design: as this has become more completely understood, emphasis has shifted to signal retrieval. Many signal processing schemes have been used and it is only recently that these fragmented approaches have been seen to emphasize different aspects of a more optimum detection approach [1,7].

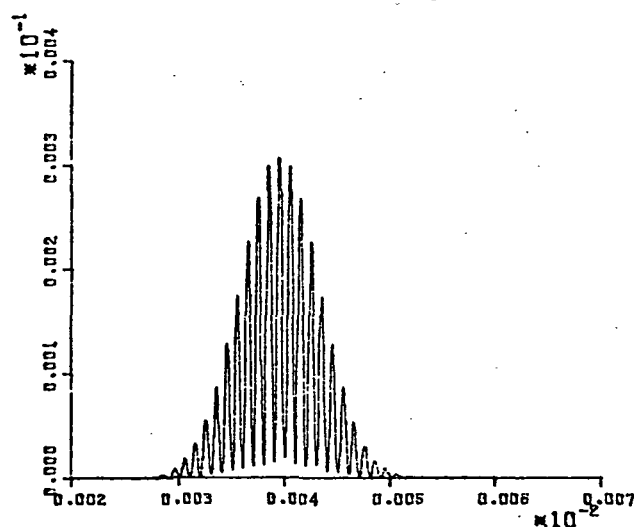
For many good reasons, the engineering difficulty or inconvenience of obtaining a classically large signal is often great and a more efficient way of transmitting and receiving scattered light and electronically detecting it has potential advantages. These may be taken as easier backscatter, greater obliquity leading to closer approach to surfaces or smaller particles. This last has further implications for the fluid dynamicist as more accurate following of the flow and more frequent estimates of velocity yield the potential for time history, as well as statistical averages in turbulence studies. This paper addresses the considerable signal sensitivity advantages of using photon correlation techniques and the further increases which are possible by using transit anemometer optics instead of fringe optics.

THE SIGNAL

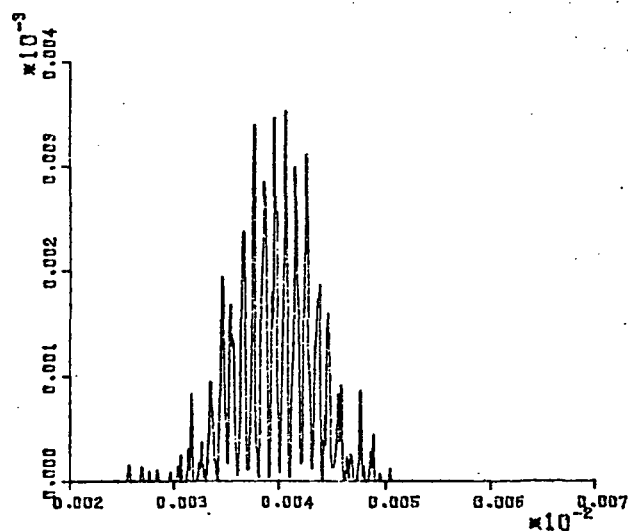
The smooth classical view of an electromagnetic wave can never be realized below infinite energy. All finite powers may be regarded in theory as a train of non-overlapping quanta (photons) and the mean rate and intervals carry all the information which may ever be extracted. A consequence of reducing signal power is the qualitative change in the nature of the pulse modulation, and this may not be reversed by later amplification back to the former power. In any real experiment, there is a limit to the smallest interval between two photons which may be resolved, and this is equivalent to low pass filtering. Reference 1 puts mathematical and quantitative rigor into these ideas and here we will review some of the new ideas which may be explored with such a generalized approach. In Figure 1, we show a computer simulation of the appearance of the signal as the energy contained within it is reduced. It shows behavior which is similar to that observed in a practical case previously published as Figure 3 of Reference 2. The signal looks dramatically different, even for the same top cut frequency of the filtering device as signal power is reduced.

Noteworthy is that the two extremes, often quoted as though they were experimental cases (Figure 1a, d) are never achieved. The 'classical' signal is never noise-free, however high the power, and the 'photon resolved' is never completely resolved because there is a certain probability of photons infinitely close together. Real signals always lie in the 'gray area' of inhomogeneous Poisson processes [1], and the only completely satisfactory approach to signal retrieval must consider how closely its assumptions approach this.

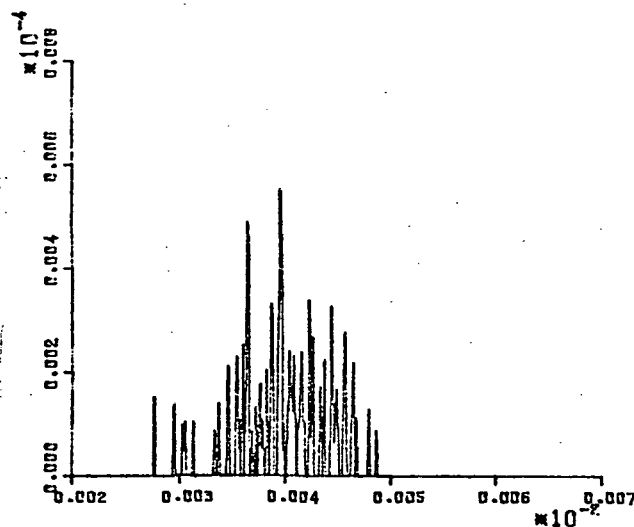
Most experiments are assumed to yield signal lying in a well defined narrow band of the above regime, but the truth is that for any real experiment, especially with polydisperse particles, the input signal may cover a very wide dynamic range in Figure 1. Many early references discussed the signal on a classical plus noise basis and more recent work has considered a quantum limited signal [3,4,5]. Both these extreme areas are amenable to good theoretical analysis and hardware conforms well to this, tracking and counting in the former case and photon correlation for very low light levels. Extensive work has been done to condition real signals into one regime or the other with questionable attention to the consequences of the conditioning.



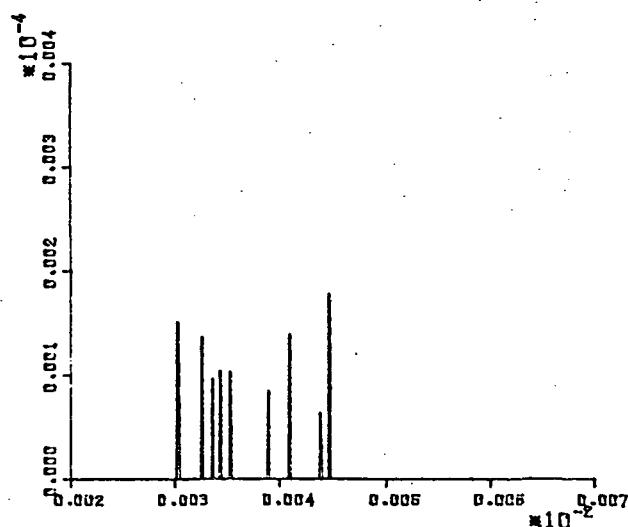
(a) Classical Signal



(b) Reduced Classical Signal



(c) Photon Limited Signal



(d) Photon Resolved Signal

Figure 1. Simulated Signals at Different Peak Power Levels.

FILTERING

Filtering is the removal of information. It may take the form of a convolution in the signal domain or a multiplication in frequency space. Its efficacy for laser anemometry relies on the separability of required information from useless 'noise' effects in the relevant space. There is always a top cut imposed by electronic component limitations and any attempt to view the signal on an oscilloscope must be after this effect. For classical interpretation, a band pass filter is applied to the signal and conventionally this must be sufficiently greater than the signal width to allow for unbiased velocity fluctuation. The alternative of a moveable filter, matched to the signal, can only be realized if a continuous estimate of center frequency is available. In the case of photon correlation, no filter is used on the signal, but correlation separates 'signal' and 'noise' effects in the correlation domain as a complex non-linear transform of the 'low frequency' signal and a smooth flat background from the Poisson noise. Again the assumption of separability is applied, this time in the correlation space and the 'noise' on the transformed data is now both photon number fluctuations and stochastic failure of the stationarity condition; i.e., if the sample of data is too short, the correlation is still not easy to extract from the variability error.

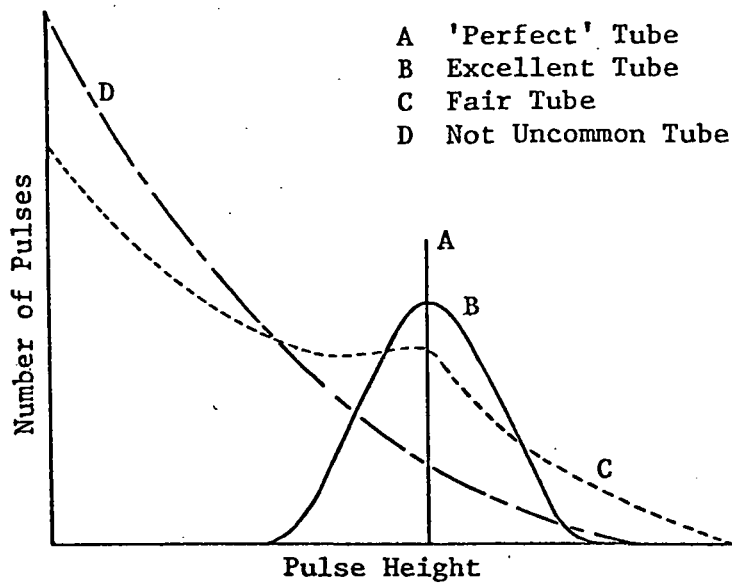


Figure 2. Photomultiplier Output Behavior from Single Photon Input.

REAL DEVICES

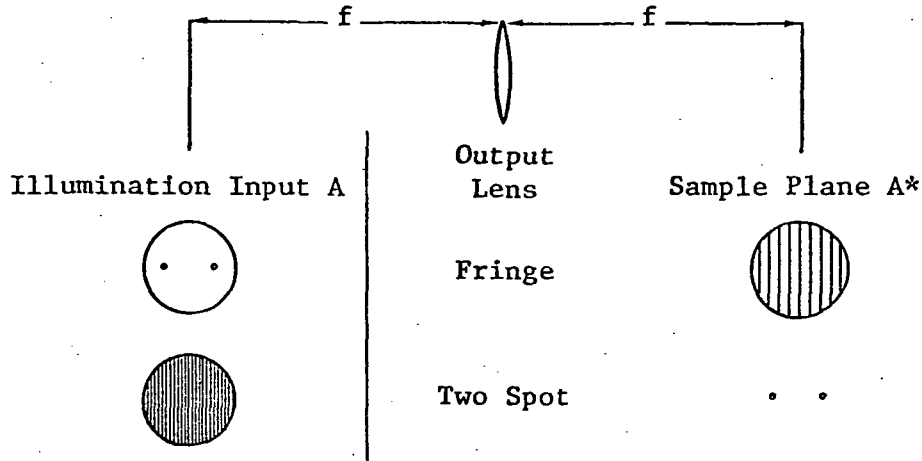
The foregoing discussion has assumed a photon detector which is imperfect only in its finite time of response, an equivalent dead time. Real photomultipliers fail on a number of other counts. The production of a discriminable pulse from every photon is not guaranteed because of limited quantum efficiency, and noise may give pulses which are discriminated as photon events. Figure 2 shows schematic performance of phototubes. For semi-classical assumptions, the tube performance is often considered not to give serious problems. For quantum resolved signals, it matters very much. Actually, it matters everywhere, but sometimes one can neglect the effects without serious consequences.

A second source of spurious events in experiments is light scattered from other than the measured particles. Although the photon statistics of this light are different, there is a limit to the way this may be used to eliminate flare effects. It is best to reject spurious light by optical design. Away from walls, this improves spatial resolution, and for a given acceptable amount of flare, enables one to work as close as possible to walls. It is not uncommon for those investigators who have only used burst counting techniques to be unaware of the severe detrimental effects of flare light. Such flare is common inside poorly designed or improperly used coaxial backscatter optical systems. This flare limits burst counting systems less than photon counting systems only due to the higher required signal levels of the classical technique.

FRINGE AND TRANSIT SYSTEMS

There is a transform relationship between these two configurations as shown in Figure 3. The discussion now reduces to the relative merits of A and A* as the better encoding operator for the scattered light. It might seem at first sight that for a fixed size of scattering center an analog of the Fellgett advantage might accrue from the two-spot encoding, but this is complicated by other geometrical features and constraints on the velocity direction sensed.

From the diagram, Figure 4, we define the sense and orientation of the fringes and spots, and proceed to describe the intensity which would be detected at any point in the sampling space. We will borrow (with minor changes) from the work of Abbiss in Reference 5 to illustrate the intensity in the fringe



A and A* related by Fourier Transform.
Diagrams not to scale.

Figure 3. Relationship of Fringe and Two Spot Illumination.

volume and use a change of notation to make the fringe and transit descriptions comparable.

In the case of a fringe system,

$$I_f(s) = k_f \exp \left[\frac{-2}{\ell_o^2} \left(x^2 \cos^2 \theta + y^2 + z^2 \sin^2 \theta \right) \right] \times \left[\exp \left(\frac{4}{\ell_o^2} x z \sin \theta \cos \theta \right) + r^2 \exp \left(\frac{-4}{\ell_o^2} x z \sin \theta \cos \theta \right) + 2r \cos \left(\frac{4\pi}{\lambda} x \sin \theta \right) \right] \quad (1)$$

where k_f is a proportionality constant.

For equal intensity beams, a case which is usable for real fringe anemometry this reduces to:

$$I_f(s) = k_f \exp \left[\frac{-2}{\ell_o^2} \left(x^2 \cos^2 \theta + y^2 + z^2 \sin^2 \theta \right) \right] \times \left[\cosh \left(\frac{2}{\ell_o^2} x z \sin 2\theta \right) + \cos \frac{4\pi}{\lambda} x \sin \frac{\theta}{2} \right] \quad (2)$$

Because this is a complicated expression, it is quite general to restrict this volume further by the receiving aperture. For small θ , leading to a highly elongated volume, the idealized truncation in the z direction is considered to reduce the expression to:

$$I_f(s) = k_f \exp \left[\frac{-2}{\ell_o^2} \left(x^2 + y^2 \right) \right] \cdot \cos \left(\frac{2\pi x \theta}{\lambda} \right) \quad (3)$$

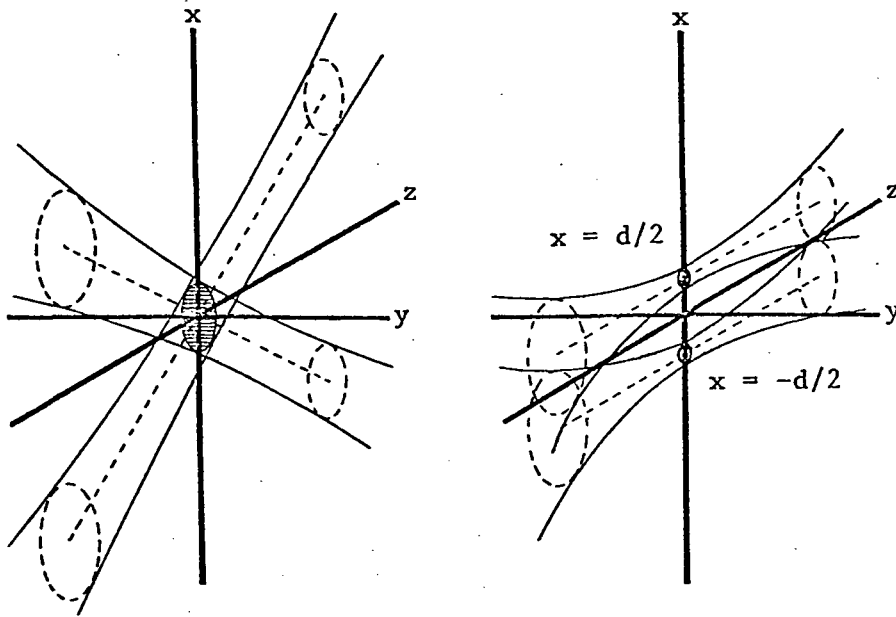


Figure 4. Schematic of Fringe and Transit Illuminated Volumes.

We show in Table 1 some typical comparative specifications for fringe and two-spot systems. Figure 5 is the simulation of the classical fringe velocimeter signal from a $0.3 \mu\text{m}$ diameter particle with the amplitude given in photoelectrons/sec. Figure 6 is the output of the photomultiplier tube. The peak mean photoelectron rate is approximately 5×10^7 , so this signal would be totally swamped by large background light. Figure 7 illustrates the classically expected pulse from one of the two spots. Figure 8 shows the PMT output. Figures 9 and 10 depict the same signal in the presence of 10^{10} photoelectrons/sec background light.

It is much more likely that one will obtain a high background from flare when using the fringe system (with a 260 micrometer diameter pinhole in the receiver) than when using a two-spot system (10.6 micrometer diameter pinhole). Thus, the two-spot system produces large signal-to-noise ratio advantages for single signals in three ways: the filter for the two-spot can be proportionately much narrower than the fringe system filter if a tracking filter is not used; the two-spot has higher intensity signals by a factor equal to the square of the ratio of the beam radii at the probe volume; the background light which will get through the pinhole spatial filter is much less for the two-spot system due to the smaller apertures. On the negative side, all optical aberrations, including those introduced by windows and turbulent index of refraction effects, will enlarge the achievable spot size and reduce the advantage of a transit velocimeter system.

For the two-spot system, the equivalent illumination intensity function may be written for Gaussian optics [6] as:

$$I_t(s) = \frac{P}{\pi W^2(z)} \left[\exp \left(\frac{-2[(x-d/2)^2 + y^2]}{W^2(z)} \right) + \exp \left(\frac{-2[(x+d/2)^2 + y^2]}{W^2(z)} \right) \right] \quad (4)$$

where P is the total power included in both beams, and $W(z)$ is the $1/e^2$ intensity radius given by

$$W(z) = W_o \sqrt{1 + \left(\frac{\lambda z}{\pi W_o^2} \right)^2} \quad (5)$$

Table 1. System Parameters.

<u>Parameter</u>	<u>Two-Spot</u>	<u>Fringe Velocimeter</u>
System		
Wavelength	514.5 nm	514.5 nm
Laser Power	0.5 watt/spot	1 watt
Optical Efficiency	0.3	0.3
Detector Quantum Efficiency	0.2	0.2
Transmitted Beam Diameter	25 mm	1 mm
Range	400 mm	400 mm
Beam Separation at Transmitter	0.5 mm \approx 0	20 mm
No. of $1/e^2$ Fringes	0	25
Probe Volume Spot Diameter	10.6×10^{-6} m	N/A
Signal Frequency	N/A	38.9 MHz
Probe Volume Width	N/A	262×10^{-6} m
Single Burst Duration	26.6×10^{-9} s	0.655×10^{-6} s
Particle		
Velocity	400 m/s	400 m/s
Index of Refraction	1.5+j0	1.5+j0
Diameter	0.3×10^{-6}	0.3×10^{-6}

Background Light

Two Levels: zero and 10^{10} photoelectrons/s
 (equivalent to 20 nw optical power collected
 by phototube)

This is not simplified by assuming a truncation function in the z direction, but neither does it change its functional form. Hence, any calculations do not depend on z selectivity. This has a shade of irony in that the conventional dimensions of use for this system do mean that it is easier to restrict sensitivity away from $z = 0$. Again, because of Gaussian beams, the z roll-off is of quasi-Gaussian form and enormously simplifies inferences in this system.

On the basis of these descriptions of the illuminated region, we now have some computer simulations of the signal appearance for each of the two systems. As might be expected, the discriminability of the signal above the noise is dramatically better for the two-spot system. The price of improvement may be reduced data rate, depending on the size distribution of scattering particles and/or it may be significantly reduced for more than a few percent turbulence because not so many particles may cross both spots as would have crossed an equivalent fringe system. Of course, this may not be a serious problem if it is a good estimate of flow direction which is required.

To summarize, the distinction between the two systems is not very tidy, but in situations where scattered light is a problem, the transit system is superior to the real fringe system. The theoretical improvement factor is up to 10^5 , but 10^2 to 10^3 is easily realized by competent optical design.

As shown by the simulations, we may use classical signal descriptions for the transit systems for much smaller scattering centers due to the concentration of light. In cases where the background flare light is kept to a reasonable value, such as 10^6 or less, much smaller signals which are photon resolved may be detected by photon correlation techniques.

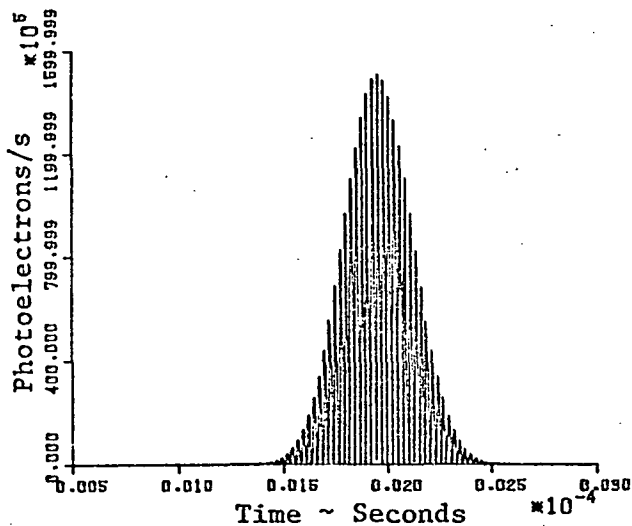


Figure 5. Classical Signal, Fringe Velocimeter.

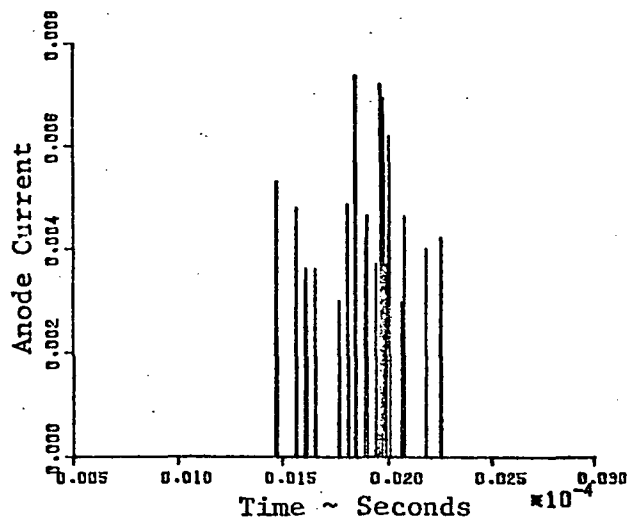


Figure 6. Photomultiplier Output, Fringe Velocimeter.

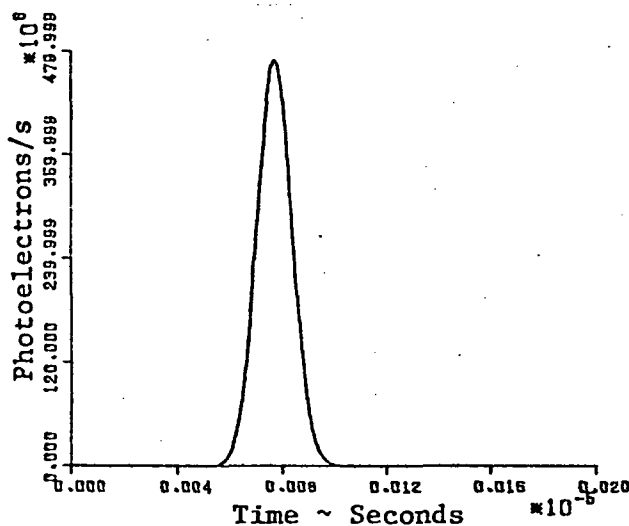


Figure 7. Classical Output, Transit Velocimeter.

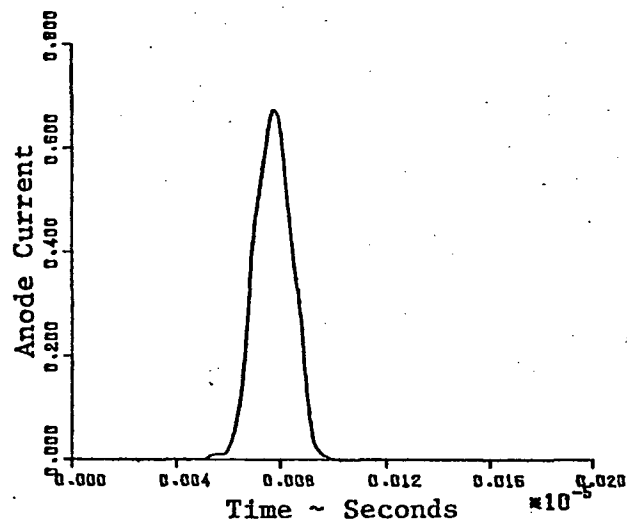


Figure 8. Photomultiplier Output, Transit Velocimeter.

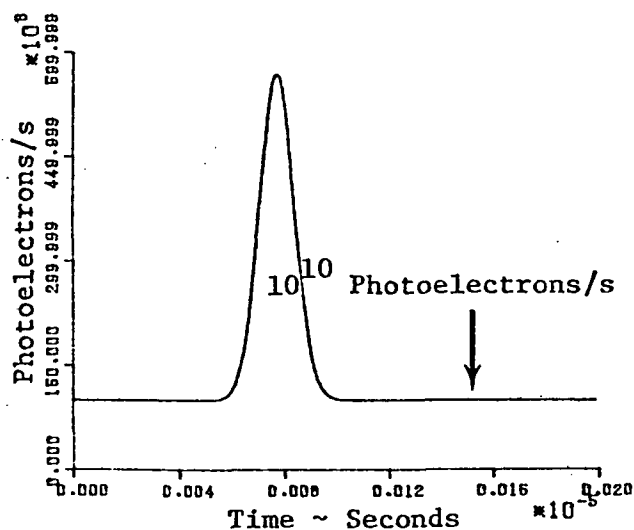


Figure 9. Transit Velocimeter, Classical Signal with Background.

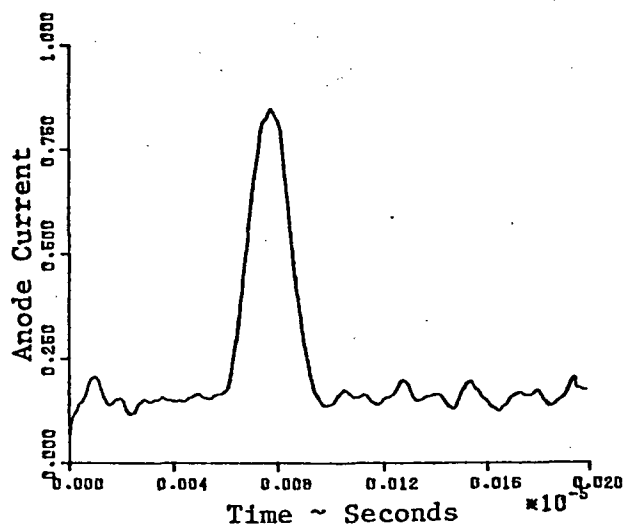


Figure 10. Photomultiplier Output, Transit Velocimeter with Background.

TRANSIT ANEMOMETER MEASUREMENTS

Several pieces of excellent work [8,9] have been reported using the advantages of the transit anemometer system. We enclose some simple examples here of the type of performance observed. Figure 11 shows a boundary layer traverse at an oblique angle onto the surface of a turbine cascade blade. The measured points were taken in random order and no difficulty was experienced with flare even as close to the surface as $100\text{ }\mu\text{m}$. Figure 12 shows the angular capability taken in a time-gated system looking between the blades in a 60" diameter fan. The speed magnitude and direction were very easily measured in a few seconds. In this system, the angle is measured to high accuracy by a method discussed in Reference 2, the figure from which is reproduced here (Figure 13). Quite obviously, it is not necessary to take so many angular points -- three is usually quite sufficient for a parabolic fit on direction. The data in this figure was from a small jet.

There are cases where this transit system may be used easily where other systems may fail. It proved easy to obtain measurement in an unseeded after-burning exhaust from an aeroengine whose conditions were in excess of 800 ms^{-1} and 2000°K with steep refractive index gradients. It is possible to minimize the effect of turbulent refractive index fluctuations in this system because the projection and collection beams are co-axial and subjected to fairly similar effects. Also, the light which forms each spot travels over substantially the same path. This transit system was designed to make measurements in high-speed axial compressors, but has proved versatile and convenient for other applications. Typical accuracy is $1/2$ percent on speed and $1/2$ degree on angle, but this may be improved with care if the higher accuracy is necessary.

CONCLUSIONS

1. The application and success of photon correlation methods has increased the dynamic range of laser anemometry signals from which good measurement may be obtained.

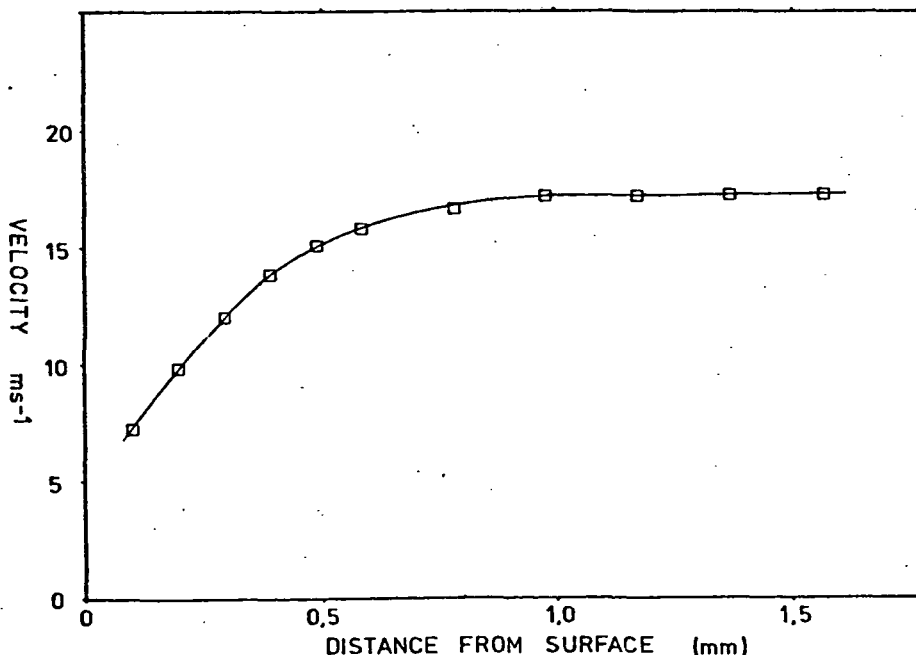


Figure 11. Boundary Layer Traverse on Pressure Surface in a Turbine Cascade.

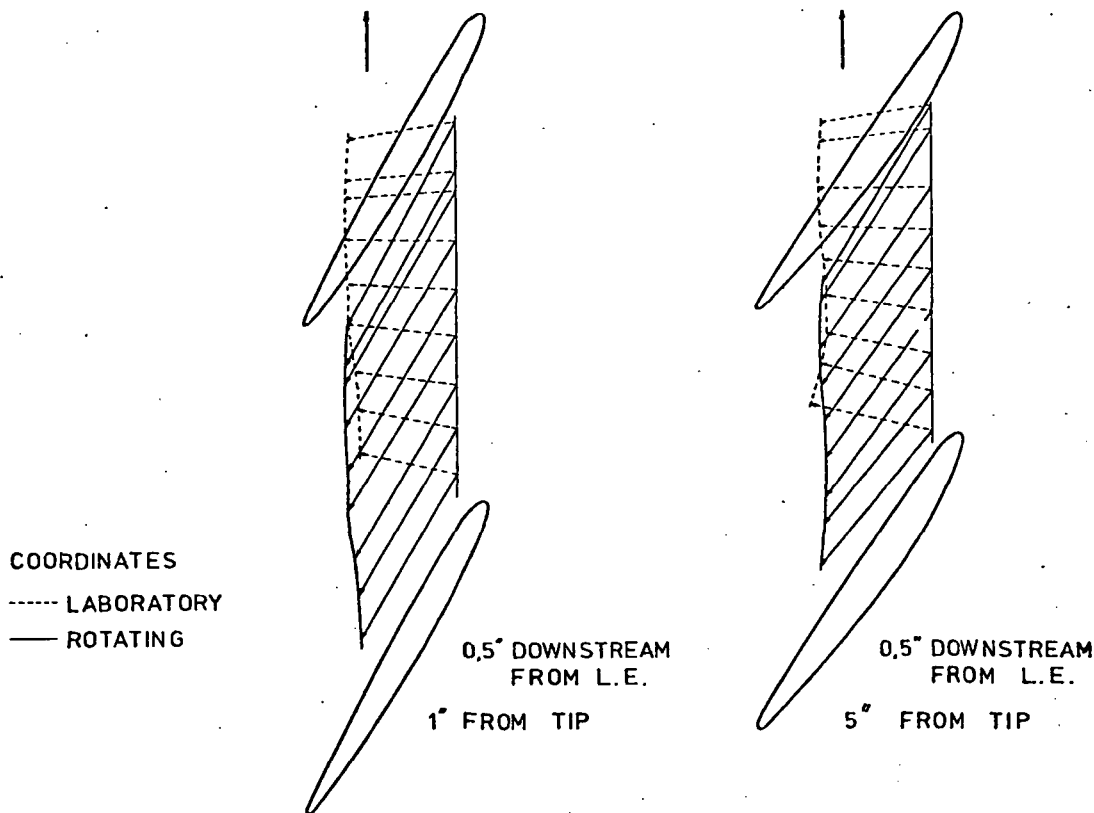


Figure 12. Inter-blade Traverses at Design Speed.

2. Explanation of these effects shows that in conditions of flare, the change to a two-spot, or transit, system is beneficial, and that the same correlation machine can be used to retrieve data in a rather different way, but with even higher rejection of noise effects.
3. While much is yet to be said and explained with the transit system, it seems to offer great promise in what have been either very difficult or impossible situations.

ACKNOWLEDGEMENTS

The comparative computer simulations were conducted by W. T. Mayo, Jr., Ms. Carolyn Greenwood and the author under U.S.A.F. Contract F040600-78-C-0002. This portion of the research was sponsored by the Arnold Engineering Development Center, Arnold Air Force Station, Tennessee, under the direction of Mr. Marshall Kingery.

The simulation programs have been developed under various research contracts with NASA Langley Research Center, the Naval Underwater Systems Center, the Advanced Research Projects Agency, and private funding by Spectron Development Laboratories, Inc.

REFERENCES

1. Mayo, W. T. Jr., "Modeling Laser Velocimeter Signals as a Triply Stochastic Poisson Process", Proceedings of Minnesota Symposium on Laser Anemometry, October 1975.

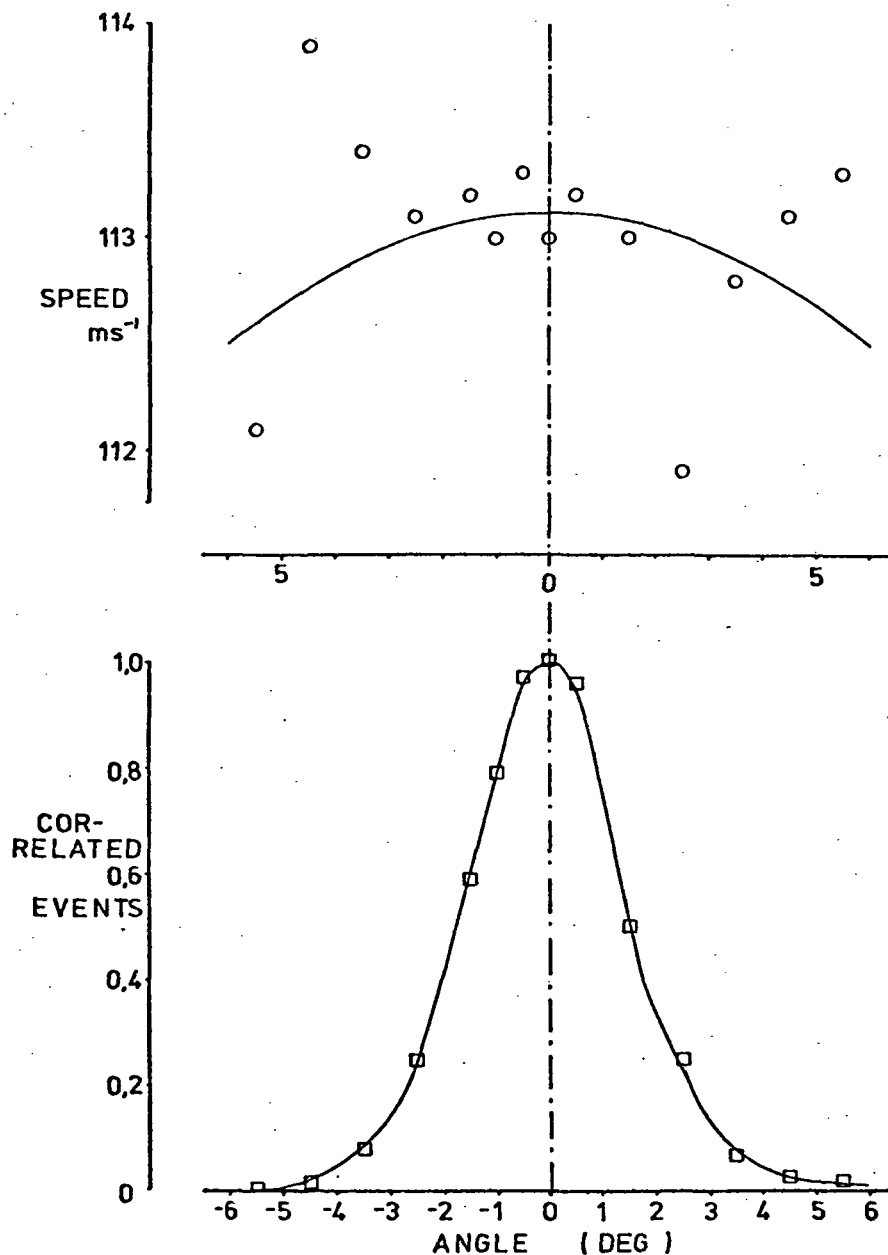


Figure 13. Direction Identification Using a Transit Anemometer.

2. Smart, A. E., "Special Problems of Laser Anemometry in Difficult Applications", Lecture 6 in AGARD LS 90, August 1977.
3. Pike, E. R. and Jakeman, E., (ed. Goodwin, D. W.), Advances in Quantum Electronics, Academic Press, 1974.
4. Cummins, H. Z. and Pike, E. R. (eds.), Photon Correlation and Light Beating Spectroscopy, NATO Advanced Study Institute, B3, Plenum, 1976.
5. Cummins, H. Z. and Pike, E. R. (eds.), Photon Correlation Spectroscopy and Velocimetry, NATO Advanced Study Institute, B23, Plenum, 1976.
6. Siegman, A. E., An Introduction to Lasers and Masers, McGraw-Hill, New York, 1971.
7. Smart, A. E. and Mayo, W. T. Jr., "Applications of Laser Anemometry to High Reynolds Number Flows", presented at the Conference on Photon Correlation Techniques in Fluid Mechanics, Stockholm, Sweden, 14-16 June 1978.

8. Schodl, R., "A Laser Dual Beam Method for Flow Measurements in Turbo-machines", ASME Paper 74-GT-157, 1975.
9. Eckardt, D., "Detailed Flow Investigations Within a High-Speed Centrifugal Compressor Impeller", ASME 76-FE-13, 1976.